Magnetic Resonance Materials in Physics, Biology and Medicine (2022) 35:277–289
https://doi.org/10.1007/s10334-021-00953-w

REVIEW

Anthropomorphic brain phantoms for use in MRI systems: a systematic review

Noelle Crasto[1,2] · **Abirami Kirubarajan**[5] · **Dafna Sussman**[1,2,3,4,6]

Received: 27 May 2021 / Revised: 13 August 2021 / Accepted: 16 August 2021 / Published online: 31 August 2021

Abstract

Objective To provide a systematic review of available brain MRI phantoms for comparison of structural and functional characteristics.

Materials and methods Phantoms were identified from a literature search using two databases including Google Scholar and PubMed. Narrow inclusion criteria were followed for identification of only tissue-mimicking MRI phantoms excluding digital, computational, or numerical phantoms. Assessment criteria for the identified phantoms was based on three categories being anatomical accuracy, tissue-mimicking materials, and exhibiting relaxation times approximating in-vivo tissues. The available features and uses of each phantom were reported and discussed using the assessment criteria.

Results Ten phantoms were identified after screening; each proposed phantom was then summarized in a table (Table 2). Significant features and characteristics were shown in the comparisons of phantom type in each category, being anthropomorphic vs. traditional phantoms. Anthropomorphic phantoms had more anatomically accurate features than traditional phantoms. On the other hand, traditional phantoms commonly used effective tissue-mimicking materials and accurate electromagnetic properties.

Discussion The findings provide an overview of the different proposed tissue-mimicking MRI brain phantoms available. Various uses and features are highlighted by comparing criteria such as anatomical accuracy, tissue-mimicking material, and electromagnetic properties. Tissue-mimicking MRI phantoms are an extremely useful tool for researchers and clinicians. Future applications include personalized phantom technology and validation of MR imaging and segmentation methods.

Keywords Brain · Magnetic resonance imaging · Phantoms · Imaging · Artifacts

Introduction

Background

Clinical magnetic resonance imaging (MRI) is used for non-invasive imaging of the body in three-dimensional detailed anatomical images. MRI has been adapted to optimize visualization of diverse components in the human body and is successfully used in the detection and monitoring of disease. MRI has excellent soft tissue contrast due to the difference in relaxation times in different tissue types [1]. Therefore, to match in-vivo results, it is usually desired that phantom materials have similar MR properties [1]. MR sequences are able to map quantitative and qualitative biomarkers; however, they require careful standardization of protocols and development of phantoms to validate in-vivo measurement, as well as to assess reliability of measurements [2, 3]. Validation and quantification of brain MRI segmentation

✉ Dafna Sussman
dafna.sussman@ryerson.ca

1 Department of Electrical, Computer, and Biomedical Engineering, Ryerson University, Toronto, ON M5B 2K3, Canada

2 Institute for Biomedical Engineering, Science and Technology (iBEST) at Ryerson University and St. Michael's Hospital, Toronto, ON M5B 1T8, Canada

3 The Keenan Research Centre for Biomedical Science, St. Michael's Hospital, Toronto, ON M5B 1T8, Canada

4 Department of Biomedical Physics, Ryerson University, Toronto, ON M5B 2K3, Canada

5 Department of Obstetrics and Gynecology, McMaster University, Hamilton, ON L8S 4L8, Canada

6 Department of Obstetrics and Gynaecology, Faculty of Medicine, University of Toronto, Toronto M5S 1A8, Canada

methods are challenging in medical image analysis, as manual validation is prone to error and is difficult to reproduce [4]. Therefore, validation of segmentation methods often requires a human-like (anthropomorphic) phantom that has electromagnetic and chemical properties that mimic in-vivo properties [4]. While homogeneous commercial phantoms are able to offer acceptable quality assurance (QA) to test MRI systems, anthropomorphic shaped phantoms go further by providing the ability to mimic a human experiment [5]. However, designing phantoms with advanced bioengineered materials to mimic the chemical and electromagnetic properties of native tissue is not straightforward. Many researchers have had little success in reproduction of the organs' inherent nature, as the goal is to reproduce the specific behaviour of the organ [4, 6].

Anthropomorphic phantoms are manufactured using materials that are equivalent to human tissues in size, shape, positioning, density, and radiofrequency interaction [5]. Tissue-mimicking MRI phantoms must have human-like qualities, and therefore, can mimic various types of biometric and physiological conditions [7]. These phantoms are also commonly fabricated in the shape of the targeted human organ, and exhibit chemical and physical stability over extended periods of time [8, 9]. Many available phantoms, however, lack realism; they poorly reflecting the shape, size, or tissue and contrast characteristics of the human brain [9]. Therefore, consistent MRI interpretation requires phantoms which allow system comparison that goes beyond basic imaging parameters, in order to provide QA as well as to test MRI performance and evaluation of new sequences and techniques [10].

Phantoms come in varying forms including physical (hardware) and numerical (software) [3]. Numerical phantoms are useful for validating and optimizing sequence parameters, but they do not mimic biophysical properties of the organ other than the specific tissue that is being simulated [3]. In this review, we will focus on hardware phantoms by identifying them as either traditional or anthropomorphic. Traditional phantoms are characterized as physical models that are traditionally manufactured, such as ones that require manual assembly or are made using household materials [11]. Traditional phantoms are frequently made using a cylindrical base and filled using tissue-mimicking (TM) liquids or gels. In this review, we characterize anthropomorphic phantoms as 3D models with a more accurate approach to an anatomically correct phantom. These models are either 3D printed or use a mold to cast a homogenous structure.

The purpose of this comprehensive review was to identify and compare available tissue-mimicking MRI phantoms, excluding digital, numerical, and computational phantoms. Simulated brain structures and tissues, simulated functions, contrast agents, and electromagnetic TM materials of each phantom were quantified. The phantoms were compared categorically as anthropomorphic or traditional phantoms. This enabled to identify the differences between these two fabrication techniques, including anatomical features, TM materials, and relaxation times. A comprehensive review of available phantoms was performed and is presented herein.

Methods

Information sources and search strategy

The literature search included the use of two databases and two alternative search methods. PubMed and Google Scholar were used as primary databases. PubMed was selected due to its advanced search feature, which can narrow search results. Google Scholar's advanced search only allows explicit terms; however, it has a broad scope of results to analyze. Alternative information sources included suggested articles in database search for appropriate literature, as well as citations within the recommended articles. All searches were conducted on Thursday, October 15th, 2020.

Three different Google Scholar searches were used as the platform only allows the user to filter words that are either explicitly included or excluded from the article or its title. This limited filtering of the literature. As a result, the search displayed articles in order of "best match" and the first 50–100 articles were screened in each search. The first search was "anthropomorphic MRI brain phantom—animal—digital" and the first 100 articles were screened. The second search was "biomimetic brain phantom (MRI OR Magnetic Resonance Imaging -digital)" and the first 50 articles were screened. The third search was "allintitle: brain imaging phantoms MRI OR MRS OR imaging—digital or—voxel or—'numerical model'".

One search was performed in PubMed; all search terms were included using the advanced search tool. Preliminary search included 'anthropomorphic brain phantoms for MRI' and then the advanced search builder was used to include the following: ('brain' or 'cerebral') AND ('MRI' or 'Magnetic Resonance Imaging' or 'MRS' or 'Magnetic Resonance Spectroscopy') AND ('phantom' or 'anthropomorphic phantom' or 'model' or 'in vitro model' or 'physical model') NOT ('mouse' or 'sheep' or 'rat' or 'rabbit' or 'primate' or 'porcine' or 'limb') NOT ('numerical model' or 'digital phantom' or 'voxel') AND (Brain imaging phantom).

The inclusion and exclusion criteria were created based on the available literature presented. Articles were not included if they were non-English articles, non-human phantoms, animal studies, not pertaining to the human brain, computational/numerical/digital phantoms, or involved non-MRI/MRS testing. Articles that were included were pertaining to MRI/MRS testing modalities, physical brain phantoms, materials mimicking average properties of the human

brain, and anthropomorphic phantom studies. Results of all search methodology and screening are illustrated in Fig. 1.

Analysis

For this review, phantoms were summarized descriptively on the basis of three key outcomes: human anatomy, TM materials, and relaxation times. These outcomes were determined a priori as the most relevant for researchers' decision-making on which phantom model to use, as based on previous literature [11].

Results

Overview of phantom models

We included ten phantom models in our review (details on individual studies are available in Table 1, study summaries

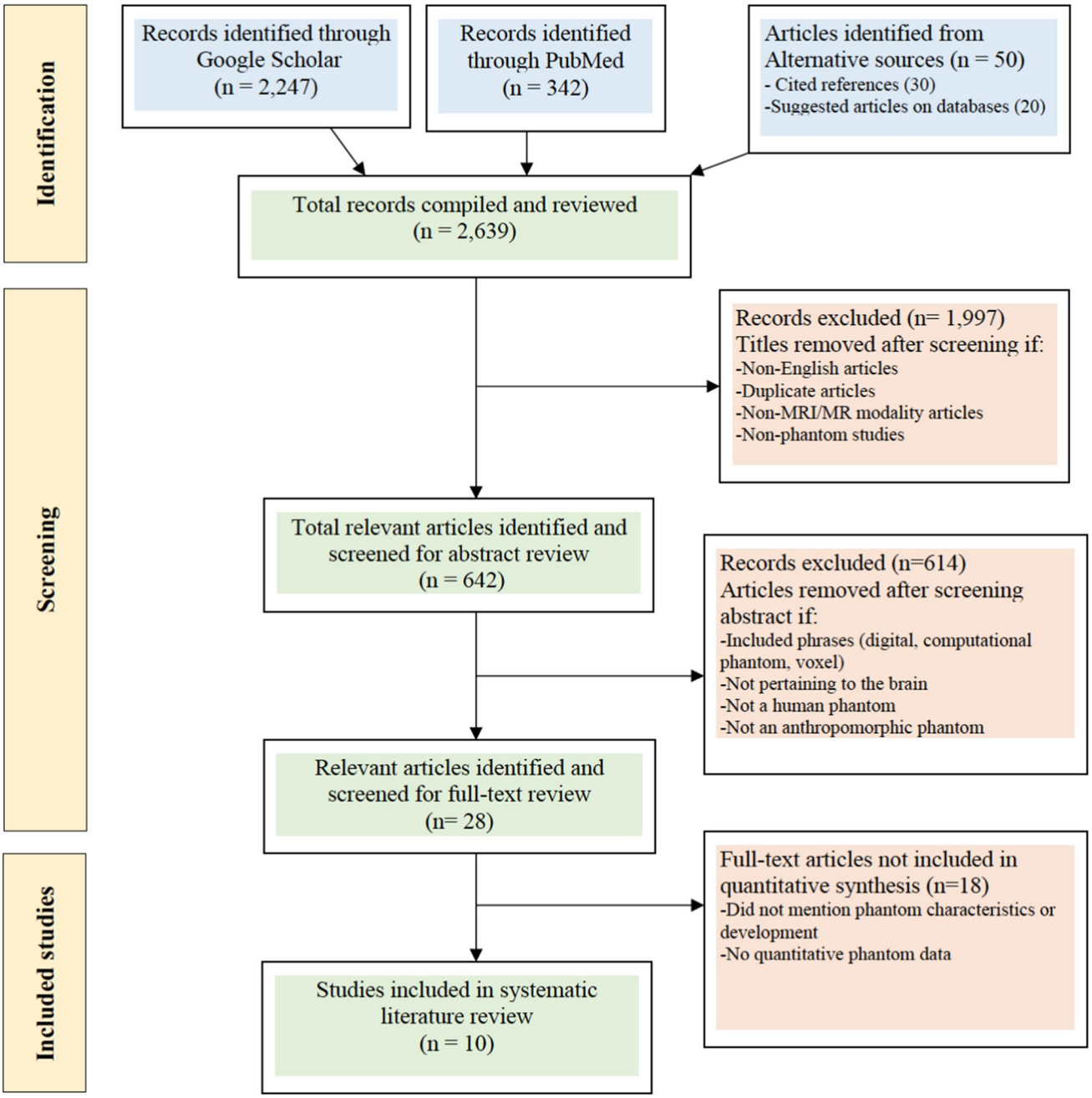

Fig. 1 Methodology of search results flowchart

Table 1 Characteristics of the identified MRI brain phantoms

Author(s)	Simulated function	Simulated structures/tissues	Contrast agents	Phantom materials used	Imaging modality	Phantom type
Rice et al. [12]	Relaxation time T1 and T2	Head phantom Brain tissues CSF Tumor tissue Ventricles	$CuCl_2$	Glass spheres and NMR tubes Gelatin/agar, 1H brain metabolites (choline, creatine, *N*-acetyl-aspartate, and lactate), NaCl, EDTA-tetra	1H MRS	Traditional phantom
Surry et al. [13]	Relaxation time T1	Brain tissues	None	Plastic mould using SLA PVA-C	MR	Anthropomorphic phantom
Shmueli et al. [14]	Relaxation time T1 and T2 B1 correction	Soft brain tissues	$MnCl_2$	Life-size anatomical plastic skull model Molten paraffin wax NaCl	MR CT	Anthropomorphic phantom
Chen et al. [15]	Relaxation time T1 and T2	Cerebral hemisphere Soft tissues Ventricles	$BaSo_4$ $CuSo_4$	Tangoplus Polyjet Resin mould using SLA PVA-C Talcum- solution	MR CT US	Anthropomorphic phantom
Khan et al. [16]	Relaxation time T1 B1 correction Volumetry-measurements	Brain ventricles surrounding-brain tissue	NaCl gadopentetate dimeglumine	Ventricle: polycarbonate using SLA Brain: TM agar	MR	Anthropomorphic phantom
Gallas et al. [17]	Relaxation time T1 and T2	Head phantom Cerebral brain- tissues Brain ventricles Tumor tissue CSF	None	Epoxy, resin for 3D printing polymerization gel- dosimeter distilled water Agarose brain metabolites	MR CT	Traditional phantom
Wood et al. [18]	Electromagnetic applications B1 mapping dielectric- measurements	Head-compartments Brain: WM, GM, external CSF, dura, brainstem tissues	None	Spherical eight compartment Cured resin material using SLA	MR	Anthropomorphic phantom
Kozana et al. [19]	Relaxation time T1 and T2	Neonatal GM and WM	Gd-DTPA	Glass vials TM agarose	MR	Traditional phantom
Altermatt et al. [20]	Relaxation time T1	GM and WM	$MnCl_2$	Silicone molds using SLA Agar	MR	Anthropomorphic phantom
Amiri et al. [21]	Relaxation time T1 Volumetry measurements	Cerebral hemisphere putamen caudate nucleus	None	Plexiglass cylinder ZP151 powder for 3D printing Water	MR	Anthropomorphic phantom

available in Table 2). All ten studies examined the MR imaging modality, with three studies also studying computed tomography and one study examining ultrasound. Seven studies manufactured anthropomorphic phantoms, while three manufactured traditional phantoms.

Purposes of phantom models

There were a range of target uses for anthropomorphic brain phantoms; the majority of the identified phantoms were able to mimic T1 and T2 relaxation times of the human tissue

Table 2 Summary of identified brain phantom studies

Year	Author(s)	Brief description of study
1998	Rice et al.	An anthropomorphic 1H MRS head phantom created using glass spheres and NMR tubes. Five different brain TM materials synthesized, including gelatin/agar mixtures with metabolites. Materials mimicked T1 and T2 of normal brain tissue (Fig. 2)
2004	Surry et al.	A PVA-C TM material for use in multiple physical phantoms including an anthropomorphic brain phantom model for use in MRI. Phantom formed using SLA and filled homogeneously. T1 relaxation in GM, WM, and muscle were found to be similar to in-vivo values. This phantom material may be appropriate for T1-weighted imaging (Fig. 3)
2007	Shmueli et al.	An anthropomorphic head phantom created using an anatomically correct plastic skull. Brain cavity was filled with MnCl solution to mimic GM and WM tissues. Paraffin wax was used to mimic soft tissues outside the brain. Tissue materials were T1 and T2 weighted similar to the human brain values (Fig. 4)
2012	Chen et al.	A realistic brain phantom created using the Colin27 dataset to accurately model sulci and insular regions of the cerebral hemisphere. PVA-C used to fill resin mold. Phantom imaged using MR T1 and T2 (Fig. 5)
2012	Khan et al.	A brain ventricle phantom created using polycarbonate digital mesh created from MR images of a subject with Alzheimer's. Ventricle was suspended in a brain mold composed of a homogeneous TM agar solution. Phantom can be used in measuring ventricle volume of Alzheimer's patients using T1 MRI modality (Fig. 6)
2015	Gallas et al.	Head phantom created using 3D printing of a head CT dataset. Phantom filled using agarose to mimic brain tissues, distilled water as CSF, and polymerization gel dosimeter for tumor surrogate. MR acquisitions of phantom included T1 and T2 (Fig. 7)
2017	Wood et al.	An anthropomorphic heterogeneous head phantom created using 3D printing. Eight compartments for phantom modeled off a male subject and segmented as tissue mesh to classify WM, GM, CSF and dura, along with other head compartments. Phantom filled with cured SLA resin material. This phantom has applications in MRI modalities (Fig. 8)
2018	Kozana et al.	Neonatal brain TM phantom simulating the MR relaxation times of neonatal GM and WM. constructed using agarose gel solutions for the optimization of T1- and T2-weighted sequences (Fig. 9)
2018	Altermatt et al.	A physical brain phantom mimicking structure and T1 relaxation properties of WM and GM using agar gel solution. Phantom shapes created using segmentation and meshes were synthesized for WM, GM and skull. Model based on the left cerebral hemisphere of a volunteer. The phantom can be used for T1-weighted MR sequence optimization (Fig. 10)
2019	Amiri et al.	Brain phantom containing three inflatable models of brain structures including cerebral hemisphere, putamen, and caudate nucleus. Models were created using 3D printing based on a post-mortem healthy brain. Phantom was filled using ZP151 powder and placed in a volume change system. Phantom analysis software can be used to induce and measure volume change of models of brain structures (Fig. 11)

with the exception of Wood et al. [18] that is optimized for the mimicking of electromagnetic properties. All these phantoms are able to accurately validate image processing techniques in MRI and four of the phantoms were manufactured for use in multiple modalities including CT as well as ultrasound.

Though the majority of studies ($n=6$) created phantoms for general brain imaging, the included studies often had specific purposes for their phantom. For example, Kozana et al. [19] noted that their phantom was specific to the neonatal brain for both grey and white matter, and provided precise results for 1.5 T MR imaging in the neonate. In contrast, Khan et al. [16] and Amiri et al. [21] created their phantoms for the purposes of assessing dementia and Alzheimer's disease, through characterization of brain atrophy as well as ventricle volumetry. Another study [17] created their phantom specifically for the purposes of ion radiotherapy and tumor mimicry.

Characteristics of phantom models

Category I: anatomical correctness

The included studies had diverse designs regarding the human anatomy of phantom models. Three of the ten studies contained both white and grey matter. Eight studies included both cerebral hemispheres, while two studies only included one hemisphere. Five studies included sulci/gyri in the model. The majority of studies included internal structures such as ventricles ($n=4$), caudate nuclei ($n=1$), or the putamen ($n=1$), while four studies omitted these anatomic landmarks. Notably, Amiri et.al. [21] provided the most complete human anatomy in their phantom model, which contained three separate inflatable models of brain structures for the cerebral hemisphere, putamen, and caudate nucleus based on both post-mortem brains as well as MR images from healthy control subjects.

The seven anthropomorphic phantoms included in this review all mimicked the anatomical structure of a brain. Accuracy was obtained using 3D molds created using patient meshes with a stereolithography apparatus (SLA) allowing precise shape and size of phantom. This technology allows

the production of shapes that resemble brain structures, such as gyri and sulci, with excellent anatomical accuracy. These complex geometries can be useful to evaluate accuracy of brain segmentation, as reported in Altermatt et al. [20]. This method was used for all anthropomorphic phantoms, with the exception of two studies. Shmueli et al. [14] used a life-sized plastic skull filled with a solution and paraffin wax as the structure instead of SLA. The B_0 field maps of this phantom were very similar to the brains of the volunteers, However, the authors proposed filling the skull with gel instead so that the phantom would have a fixed position independent of the phantom's orientation. Amiri et al. [21] phantom was 3D printed using ZP151 powder, dipped in latex rubber, and then dissolved in water. The phantom structure provided accurate volume change measurements within MR scanners. In contrast, the studies employing traditional phantoms reported that more realistic anatomies would be beneficial. For example, Gallas et al. [17] concluded that future developments should include more realistic matrices and differentiated materials, which will enable optimization of MRI soft tissue contrast.

Category II: TM materials

Common materials for phantom construction included PVA-C [13, 15], agar/agarose [12, 16, 17, 20, Konzana et al.] and resin material [15, 18, Galls et al.], with glass or plexiglass also used for tubes or spheres [12, 19, 21]. Other materials included molten paraffin wax [14] and ZP1D1 powder for 3D printing [21] (Table 1).

The studies had varying definitions regarding TM properties, as only seven studies explicitly described their methodology for mimicking human tissue, three studies did not include this [14, 18, 21]. Many of the available anthropomorphic phantom models were constructed using homogenous materials such as PVA-C, paraffin wax, latex rubber, or homogeneous solutions, which could not represent both white and grey matter [13, 15, 16, 21] (Table 1). For example, one study [15] noted that their phantom only allowed for homogeneously simulated tissue with discrete punctuate insertions, and that their model could be improved by simulating different tissues such as cortical matter or blood vessels. As such, three traditional phantoms [12, 17, 19] and two anthropomorphic phantoms [18, 20] included different TM material mimicking white and grey brain matter, including external CSF, dura, cerebellum, and brainstem tissues. The traditional phantoms mentioned above, exhibited segmented brain compartments consisting of appropriate TM materials including white matter, grey matter, as well as metabolites of interest. Rice et al. used segmented chambers to represent different brain regions, CSF, as well as simulated tumours. This is similar to Gallas et al. that used chambers to represent the brain tissue surrogate, cerebrospinal fluid, and polymerization gel dosimeter. Kozana et al. used organized glass vials to mimic specific TM material concentrations found in the neonatal brain.

Stability of TM materials was reported in four of the included studies [12, 13, 19, 20], with the exception of creatine, which was susceptible to rapid degradation. In Rice et al., there was no change in the NMR spectra of the relaxation properties of the traditional phantom over 2 years. Similarly, Kozana et al. reported long-term stability of the traditional phantom over a 12-month period with less than 5% coefficient variation for T1 and T2 relaxation. Short-term stability was featured in the anthropomorphic phantom constructed by Altermatt et al. with tests of structural stability and relaxation properties over a 28-day period. In other anthropomorphic phantoms that did not explicitly include statements on longevity, such as Khan et al., studies reported that it is possible to easily use refrigeration and add preserving agents to agar solutions to prolong shelf life.

Category III: relaxation times

Relaxation times were noted as an outcome in nine studies, except by Wood et al. [18], who did not measure T1 or T2. All studies that did measure relaxation were successfully validated as similar to real tissues. Six studies mimicked the relaxation time of all individual tissues being simulated. Three studies mimicked relaxation time through theoretical calculations. Five studies measured T1 and T2, while the four remaining studies only included applications that used T1 measurements (Table 1). Most reported relaxation times were able to mimic that of native tissue for both traditional [Kozana et al., 19] and anthropomorphic [14, 16, 20] models. For example, Rice et al. [12] noted that their traditional phantom's relaxation time compared well with a pig brain. However, Chen et al. [15] anthropomorphic phantom did not match the T1 relaxation time for their brain tissue, which Khan et al. [16] noted may be due to the limited anatomy (e.g., single hemisphere, half of the left ventricle) modelled. Of note, Gallas et al. [17] noted that T2 and, to a smaller degree, T1 MR relaxation times can be altered through modifying the agarose composition of the gel material.

Many of the following studies also used contrast agents in their phantoms to modify the relaxation time of TM material (specific contrast agents available in Table 1). The most common contrast agents included $MnCl_2$ ($N=2$) and gadolinium ($N=2$), while four studies did not report use of a contrast agent [13, 17, 18, 21]. There were noted challenges of contrast agents for phantom models. For example, Altermatt et al. [20] noted that the diffusion of a contrast agent reduced the longevity of a phantom, and that caution was required. Similarly, Chen et al. [15] noted that the copper sulfate agents often leaked from the landmark structures into the surrounding tissue. Chen et al. [15] proposed that

this challenge could be circumvented by sealing landmark structures, though this was not formally tested. Another study also noted potential constraints of rapid freeze–thaw cycles as artefacts can be created through local thawing [13], yet, other studies with freeze–thaw cycles did not note this concern.

Discussion

In this review, ten brain MRI phantoms were identified and summarized descriptively on the basis of three key characteristics: human anatomy, TM materials, and relaxation times.

Category I: anatomical correctness

The shape of anthropomorphic phantoms allows more accurate structural models of the human brain in comparison to traditional phantoms with generalized shapes. This structural progression over the traditional brain phantom is largely attributed to the use of 3D printing molds. Stereolithography (SLA) was the most common printing technique for creation of 3D brain molds among the anthropomorphic phantoms reviewed. Patient MRI scans are segmented and printed as brain molds to obtain complex anatomical features, such as the accurate shape and size of the brain, the complex structure of the sulci and gyri. This approach is cost and time-effective and allows creation of more complex and detailed phantoms [22]. Some phantoms using this method were only created for one cerebral hemisphere. These often do not accurately mimic a human brain nor result in an accurate image due to phantom positioning within the RF coil, which is different from a human brain [20]. However, the field is rapidly evolving. Advances in complexity of brain phantoms make them optimal for imaging or dosimetry measurements [22]. Anthropomorphic head phantoms, however, are often simple in shape and only offer an acceptable quality assurance to test signal-to-noise-ratio of the MRI system. In our review, this was also true for the brain component of head phantoms. However, one of the phantoms created by Wood et al. had a simplified anatomical structure which mimicked multiple anatomical brain features using 3D-printed molds from patient MRI scans. This demonstrates that anthropomorphic brain models could be made using patient MRI scans to mimic anatomical brain structures using. On the other hand, traditional phantoms are often restricted to simple geometries, such as spheres filled with a solution containing metabolites. These models have limited capacity for assessing spatial characteristics [23]. An anatomically accurate brain must include external and internal structures including deep cortical structures and ventricles.

Category II: TM materials

Many of the available anthropomorphic phantom models were constructed using homogenous materials such as PVA-C, paraffin wax, latex rubber, or homogeneous solutions, which could not represent both white and grey matter [13, 15, 16, 21]. A heterogeneous phantom is needed to accurately represent all soft tissue in the brain, including the surrounding CSF. Traditional phantoms exhibited segmented brain compartments consisting of appropriate TM materials which included the metabolites of interest. However, such metabolites were not included in all phantoms, as this feature is mostly useful for MRS purposes. In brain MRI, there have not been a large number of anthropomorphic phantoms developed that exhibit increased similarity of the human patient in both tissue properties as well as anatomical shape. One exception is phantoms such as the one by Altermatt et al., which exhibited both features [20]. Therefore, a greater emphasis on incorporating TM materials in anthropomorphic MRI brain phantoms is needed to improve their accuracy and utility.

Category III: relaxation times

Many anthropomorphic phantoms only mimicked either T1 or T2 relaxation times of the simulated tissues. Yet, it is important that both relaxation times are mimicked to be able to test quantitative MR sequences [24]. This may be attributed to the acquisition of reference MRI patient scans, and unique purposes of the phantom study. Phantoms that are purposed for identification or quantification of disease and disease progression are optimized for the pulse sequence that best captures the targeted condition. However, a phantom that has both features can be used to test sequences for a more versatile range of conditions. T1-weighted MRI is used to capture high signal frequency of inflammatory tissues or malignancies. On the other hand, T2-weighted MRI is used in pathology to detect edemas or irregular tissue growth [25, 26]. The most versatile phantoms were found to be those using paramagnetically doped agar or agarose gels, which mimicked both T1 and T2 values [27]. T1 relaxation times could be modulated by adding paramagnetic ions, while T2 could be modulatedby changing the concentrations of the gelling agent [10, 27, 28]. Nonetheless, many anthropomorphic phantoms were found to not mimic tissue T2 values due to the risk of compromising the physical strength of the phantom [28]. As an alternative solution, materials such as carrageenan have been found to provide the phantom with sufficient structural strength without greatly affecting relaxation times [28]. To increase the accuracy of MRI brain phantoms there should be greater emphasis on development of TM materials that mimic both T1 and T2 tissue relaxation

times. This will ensure appropriate and benefit the development of versatile use in MR phantoms.

Recommendations

Ultimately, it is important for each phantom to be designed with a specific goal and context in mind. Currently, available phantoms succeed in their purported goals, but there have been a number of goals from which appropriate phantoms have not yet been constructed due to technical limitations. Specifically, the identified phantoms in this review offer strengths in different areas; traditional phantoms offer the highest accuracy for TM materials and relaxation time but lack anatomical accuracy. Future phantoms should look in the direction of physical models with better TM material that simulate T1 as well as T2 properties. In addition, an important property that was not featured in these models is appropriate conductivity of the phantom materials. Dielectric properties and conductivity measurements were only found in one phantom [19]. This feature is important for the phantom to accurately mimic the electromagnetic properties of biological tissue in a real patient MR environment [8]. Testing of chemical and physical stability over time was not discussed in many of the reviewed phantoms and is a required feature to authenticate the precision and reproducibility of the measured parameters [3, 8, 9]. As this field moves towards customized phantoms for versatile MR sequencing, the time required for prototyping and fabrication of phantoms, as well as the associated costs, remain limiting factors [23]. Future research in brain phantom imaging should investigate phantom customization and reproduction of a variety of conditions and procedures using quantitative MRI, as was featured in the Khan et al. [16] and Amiri et al. [21] phantoms. These phantoms were optimized for use in volumetry studies for patients with neurodegenerative disorders [29]. An example of personalized phantom technology can include tailored procedures such as MR thermometry in ischemic stroke patients. TM materials could also mimic specific heat capacity, density, and relative dielectric permittivity of in-vivo brain tissues [30]. MR thermometry is a procedure that can be applied through anthropomorphic brain and head phantoms in the future [18]. Minimally invasive thermal therapy of benign and malignant diseases is able to benefit from near real-time MR image guidance [31]. Developing phantom technology that accurately mimics malignant diseases with tissue contrast for temperature mapping would enable quality assurance for these therapies [19].

Review limitations

Our review only identified anatomical phantoms and did not include digital, computational, or numerical phantoms. Future reviews may wish to broaden the scope of the inclusion criteria to include these phantoms and evaluate the differences between the development of the technologies. This will better support clinicians in choosing the appropriate technologies for target uses, and aid developers in identifying strengths and challenges to improve upon in current technologies.

Conclusion

Tissue-mimicking MRI phantom models exhibited differences in characteristics when compared by synthesis type being traditional or anthropomorphic. Anthropomorphic phantoms are able to mimic the anatomical shape and size of an MR patient scan more effectively than traditional phantoms with the development of 3D printing technology for phantom moldings and artifacts. Traditional phantoms exhibit more accurate TM material for all brain tissues including grey matter, white matter, and CSF. Moreover, traditional phantoms are increasingly accurate in exhibiting appropriate T1 and T2 relaxation times for the simulated brain tissues than anthropomorphic phantoms. To further facilitate personalized phantom technology and validation of brain image segmentation algorithms, future developments should be aimed at producing phantoms having the anatomical accuracy of current anthropomorphic phantoms, while employing and optimizing materials that mimic tissues and relaxation times like current traditional phantoms.

Appendix

See Figs. 2, 3, 4, 5, 6, 7, 8, 9, 10 and 11.

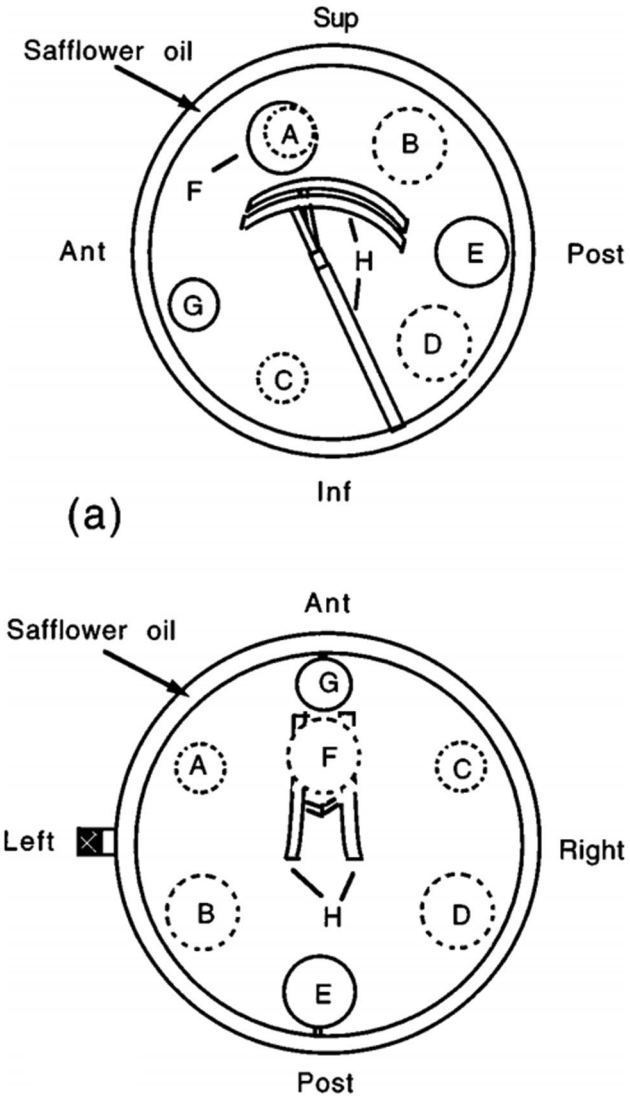

Fig. 2 Diagrams of sagittal (top) and axial (bottom) views of head phantom developed by Rice et al. [12]. Reprinted with permission from John Wiley and Sons: Rice et al. [12]

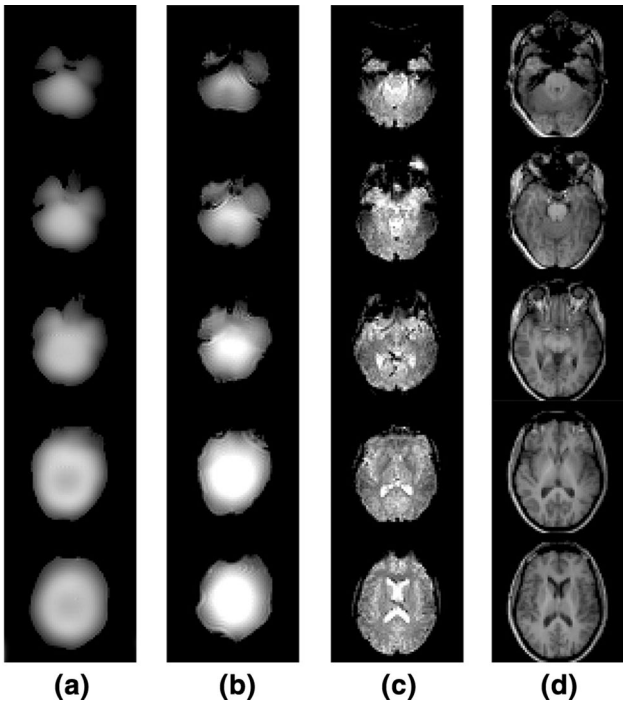

Fig. 4 GE-EPI MRI images of transverse slices from anthropomorphic brain phantom. Slices from an SE image of the phantom (**a**), GE-EPI scans of phantom (**b**), GE-EPI volunteer scans (**c**), and 3D structural scan of volunteer (**d**). Developed by Shmueli et al. [14]. Reprinted with permission from John Wiley and Sons: Shmueli et al. [14]

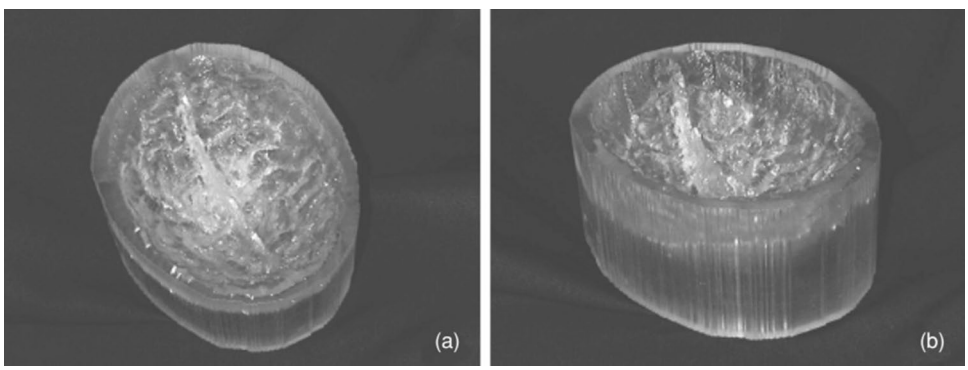

Fig. 3 Brain phantom SLA mould top (**a**) and side view (**b**) developed by Surry et al. [13]. © Institute of Physics and Engineering in Medicine. Reproduced by permission of IOP Publishing. All rights reserved. Surry et al. [13]

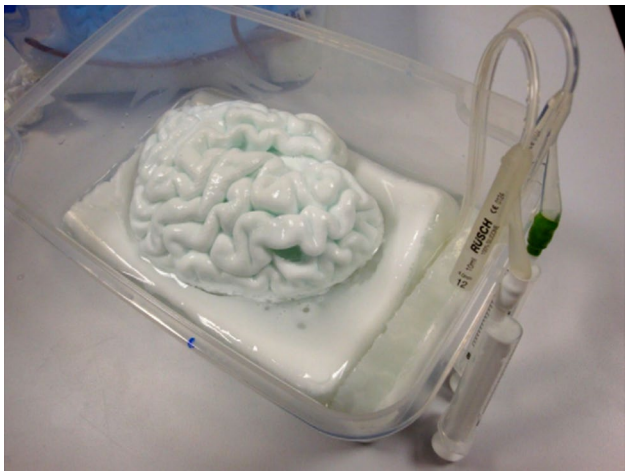

Fig. 5 PVA-C brain phantom casted from Colin27-based phantom mold developed by Chen et al. [15]. Permission to reprint granted by John Wiley and Sons: Chen et al. [15]

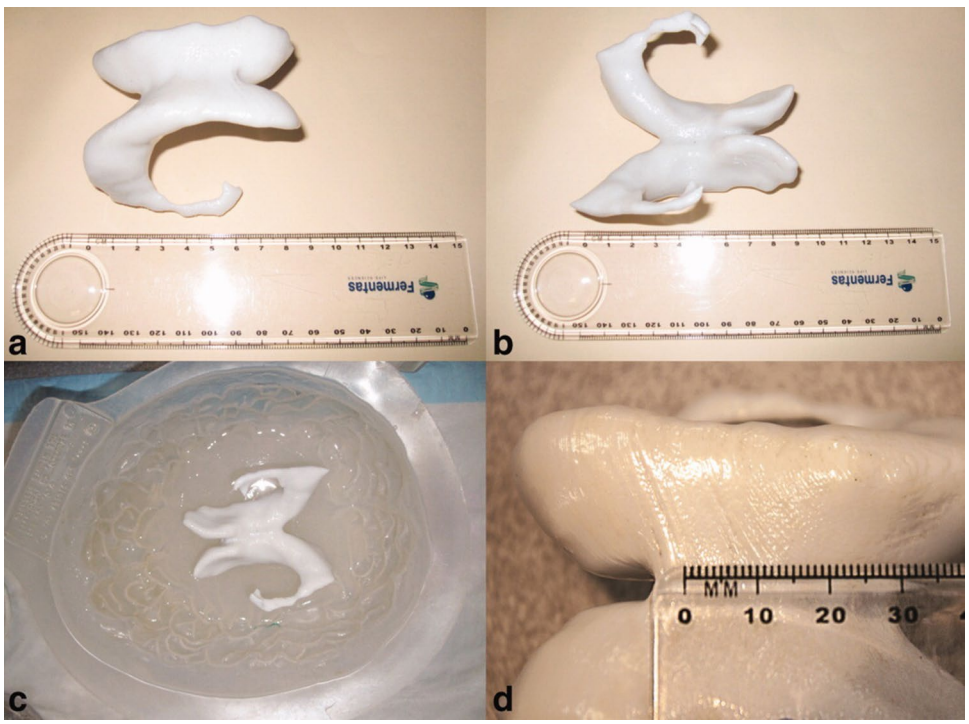

Fig. 6 Brain phantom with fabricated ventricle (**a**–**c**). Ventricle demonstrating proper base for mid-brain positioning (**d**). Developed by Khan et al. [16]. Reprinted with permission by John Wiley and Sons: Khan et al. [16]

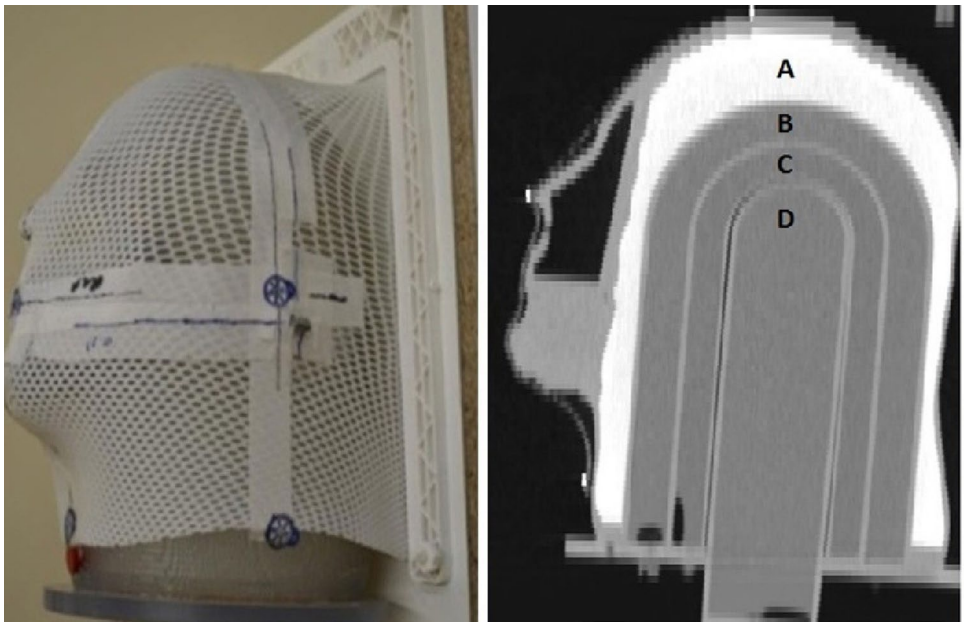

Fig. 7 Head phantom prototype (left). CT image (right) with cranial bone surrogate (**a**), brain tissue surrogate (**b**), CSF surrogate (**c**), and polymerization gel dosimeter (**d**) developed by Gallas et al. [17]. Reprinted with permission of Elsevier: an anthropomorphic multimodality (CT/MRI) head phantom prototype for end-to-end tests in ion radiotherapy, 2015

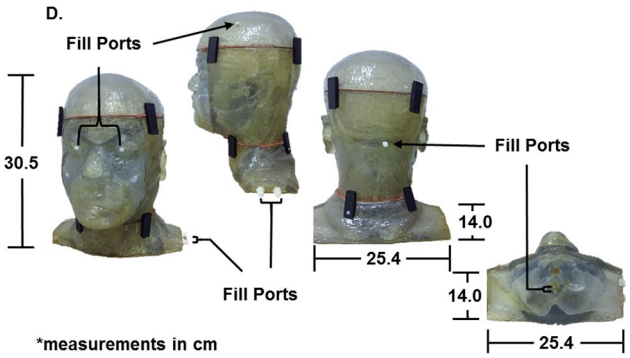

Fig. 8 Heterogeneous anthropomorphic head phantom model with fill ports for tissue-mimicking materials developed by Wood et al. [18]

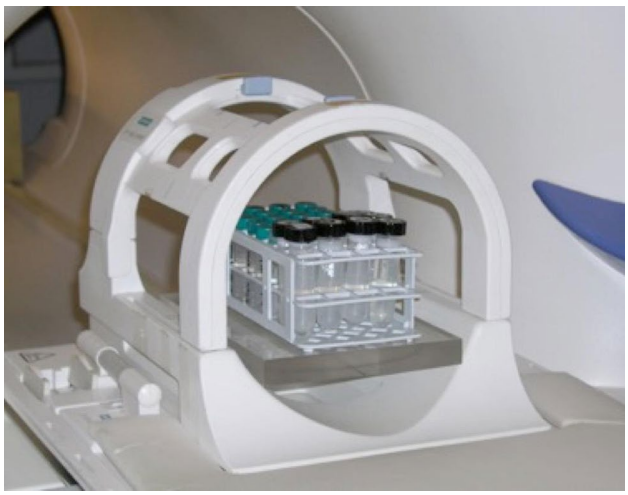

Fig. 9 Neonatal brain tissue-mimicking phantom positioned inside the adult head coil developed by Kozana et al. [19]. Reprinted with permission from Elsevier: Kozana et al. [19]

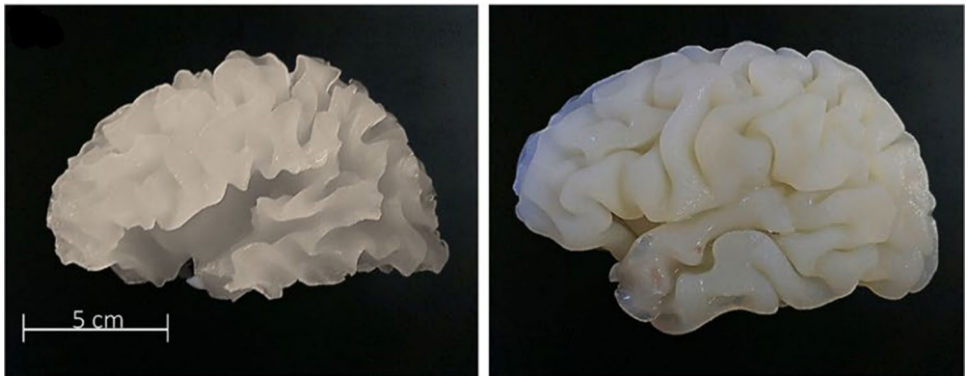

Fig. 10 Brain phantom created by silicone molds. White matter gel (left), and grey matter (right) additionally containing the white matter gel developed by Altermatt et al. [20]. Reprinted with permission from John Wiley and Sons: Altermatt et al. [20]

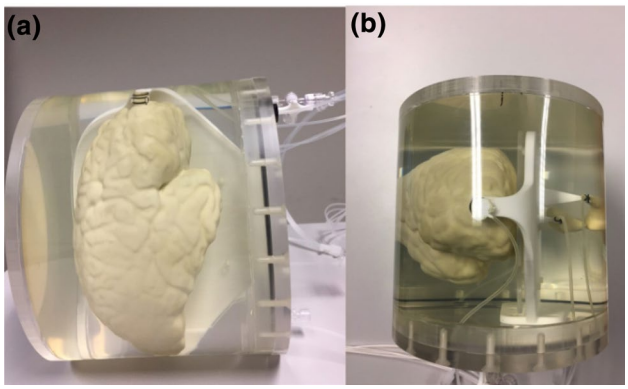

Fig. 11 Side (**a**) and top view (**b**) of brain phantom in volume change system developed by Amiri et al. [21]

Author contributions NC conducted the literature search, screening, literature review. NC and AK interpreted data and drafted the manuscript. DS conceived the study, supervised and funded the research, and edited the manuscript for publication.

Declarations

Conflict of Interest The authors declare no conflict of interest.

References

1. Valladares A, Beyer T, Rausch I (2020) Physical imaging phantoms for simulation of tumor heterogeneity in PET, CT, and MRI: an overview of existing designs. Med Phys 47(4):2023–2037. https://doi.org/10.1002/mp.14045
2. Keenan KE et al (2018) Quantitative magnetic resonance imaging phantoms: a review and the need for a system phantom. Magn Reson Med 79(1):48–61. https://doi.org/10.1002/mrm.26982
3. Fieremans E, Lee HH (2018) Physical and numerical phantoms for the validation of brain microstructural MRI: a cookbook. Neuroimage 182:39–61. https://doi.org/10.1016/j.neuroimage.2018.06.046
4. Despotović I, Goossens B, Philips W (2015) MRI segmentation of the human brain: challenges, methods, and applications. Comput Math Methods Med. https://doi.org/10.1155/2015/450341
5. Medeiros Oliveira Ramos S, Thomas S, Bárbara Torres Berdeguez M, Vasconcellos de Sá L, Augusto Lopesde Souza S (2017) Anthropomorphic phantoms—potential for more studies and training in radiology. Int J Radiol Radiat Ther. https://doi.org/10.15406/ijrrt.2017.02.00033
6. Forte AE, Galvan S, Manieri F, Rodriguez y Baena F, Dini D (2016) A composite hydrogel for brain tissue phantoms. Mater Des 112:227–238. https://doi.org/10.1016/j.matdes.2016.09.063
7. Winslow JF, Hyer DE, Fisher RF, Tien CJ, Hintenlang DE (2009) Construction of anthropomorphic phantoms for use in dosimetry studies. J Appl Clin Med Phys 10(3):195–204. https://doi.org/10.1120/jacmp.v10i3.2986
8. Kato H et al (2005) Composition of MRI phantom equivalent to human tissues. Med Phys 32(10):3199–3208. https://doi.org/10.1118/1.2047807
9. Droby A et al (2015) A human post-mortem brain model for the standardization of multi-centre MRI studies. Neuroimage 110:11–21. https://doi.org/10.1016/j.neuroimage.2015.01.028
10. Hellerbach A, Schuster V, Jansen A, Sommer J (2013) MRI phantoms—are there alternatives to agar? PLoS ONE 8(8):e70343. https://doi.org/10.1371/journal.pone.0070343
11. Shulman M et al (2020) Quantitative analysis of fetal magnetic resonance phantoms and recommendations for an anthropomorphic motion phantom. Magn Reson Mater Phys Biol Med 33(2):257–272. https://doi.org/10.1007/s10334-019-00775-x
12. Rice JR, Milbrandt RH, Madsen EL, Frank GR, Boote EJ, Blechinger JC (1998) Anthropomorphic 1H MRS head phantom. Med Phys 25(7):1145–1156. https://doi.org/10.1118/1.598306
13. Surry KJM, Austin HJB, Fenster A, Peters TM (2004) Poly(vinyl alcohol) cryogel phantoms for use in ultrasound and MR imaging. Phys Med Biol 49(24):5529–5546. https://doi.org/10.1088/0031-9155/49/24/009
14. Shmueli K, Thomas DL, Ordidge RJ (2007) Design, construction and evaluation of an anthropomorphic head phantom with realistic susceptibility artifacts. J Magn Reson Imaging 26(1):202–207. https://doi.org/10.1002/jmri.20993
15. Chen SJ-S et al (2012) An anthropomorphic polyvinyl alcohol brain phantom based on Colin27 for use in multimodal imaging. Med Phys 39(1):554–561. https://doi.org/10.1118/1.3673069
16. Khan AF, Drozd JJ, Moreland RK, Ta RM, Borrie MJ, Bartha R (2012) A novel MRI-compatible brain ventricle phantom for validation of segmentation and volumetry methods. J Magn Reson Imaging 36(2):476–482. https://doi.org/10.1002/jmri.23612
17. Gallas RR, Hünemohr N, Runz A, Niebuhr NI, Jäkel O, Greilich S (2015) An anthropomorphic multimodality (CT/MRI) head phantom prototype for end-to-end tests in ion radiotherapy. Zeitschrift fur medizinische Physik,25(4):391–399. https://doi.org/10.1016/j.zemedi.2015.05.003

18. Wood S et al (2017) Design and fabrication of a realistic anthropomorphic heterogeneous head phantom for MR purposes. PLoS ONE 12(8):e0183168. https://doi.org/10.1371/journal.pone.0183168
19. Kozana A, Boursianis T, Kalaitzakis G, Raissaki M, Maris TG (2018) Neonatal brain: fabrication of a tissue-mimicking phantom and optimization of clinical T1w and T2w MRI sequences at 1.5 T. Phys Medica 55:88–97. https://doi.org/10.1016/j.ejmp.2018.10.022
20. Altermatt A et al (2019) Design and construction of an innovative brain phantom prototype for MRI. Magn Reson Med 81(2):1165–1171. https://doi.org/10.1002/mrm.27464
21. Amiri H, Brouwer I, Kuijer JPA, de Munck JC, Barkhof F, Vrenken H (2019) Novel imaging phantom for accurate and robust measurement of brain atrophy rates using clinical MRI. NeuroImage Clin 21:101667. https://doi.org/10.1016/j.nicl.2019.101667
22. Filippou V, Tsoumpas C (2018) Recent advances on the development of phantoms using 3D printing for imaging with CT, MRI, PET, SPECT, and ultrasound. Med Phys 45(9):e740–e760. https://doi.org/10.1002/mp.13058
23. Kasten JA, Vetterli T, Lazeyras F, Van De Ville D (2016) 3D-printed shepp-logan phantom as a real-world benchmark for MRI. Magn Reson Med 75(1):287–294. https://doi.org/10.1002/mrm.25593
24. Keenan K, Stupic KF, Boss MA, Russek SE (2015) Standardized phantoms for quantitative cardiac MRI. J Cardiovasc Magn Reson 17(1):1–2. https://doi.org/10.1186/1532-429X-17-S1-W36.
25. Gupta N, Khanna P (2017) A non-invasive and adaptive CAD system to detect brain tumor from T2-weighted MRIs using customized Otsu's thresholding with prominent features and supervised learning. Signal Process Image Commun 59:18–26. https://doi.org/10.1016/j.image.2017.05.013
26. Bloem JL, Reijnierse M, Huizinga TWJ, Van Der Helm Van Mil AHM (2018) MR signal intensity: staying on the bright side in MR image interpretation. Open 4:728. https://doi.org/10.1136/rmdopen-2018-000728
27. Yoshimura K et al (2003) Development of a tissue-equivalent MRI phantom using carrageenan gel. Magn Reson Med 50(5):1011–1017. https://doi.org/10.1002/mrm.10619
28. Hattori K et al (2013) Development of MRI phantom equivalent to human tissues for 3.0-T MRI. Med Phys. https://doi.org/10.1118/1.4790023
29. Maclaren J, Han Z, Vos SB, Fischbein N, Bammer R (2014) Reliability of brain volume measurements: a test–retest dataset. Sci Data 1(1):1–9. https://doi.org/10.1038/sdata.2014.37
30. Tarasek MR et al (2014) Validation of MR thermometry: method for temperature probe sensor registration accuracy in head and neck phantoms. Int J Hyperth 30(2):142–149. https://doi.org/10.3109/02656736.2014.887794
31. Rieke V, Pauly KB (2008) MR thermometry. J Magn Reson Imaging 27(2):376–390. https://doi.org/10.1002/jmri.21265